

First Observation of the Decay $B_c^+ \rightarrow J/\psi \pi^+ \pi^- \pi^+$

R. Aaij *et al.**

(LHCb Collaboration)

(Received 31 March 2012; published 19 June 2012)

The decay $B_c^+ \rightarrow J/\psi \pi^+ \pi^- \pi^+$ is observed for the first time, using 0.8 fb^{-1} of pp collisions at $\sqrt{s} = 7 \text{ TeV}$ collected by the LHCb experiment. The ratio of branching fractions $\mathcal{B}(B_c^+ \rightarrow J/\psi \pi^+ \pi^- \pi^+)/\mathcal{B}(B_c^+ \rightarrow J/\psi \pi^+)$ is measured to be $2.41 \pm 0.30 \pm 0.33$, where the first uncertainty is statistical and the second is systematic. The result is in agreement with theoretical predictions.

DOI: [10.1103/PhysRevLett.108.251802](https://doi.org/10.1103/PhysRevLett.108.251802)

PACS numbers: 13.25.Hw, 12.39.St, 14.40.Nd

The B_c^+ meson is the ground state of the $\bar{b}c$ quark pair system [1]. Studies of its properties are important, since it is the only meson consisting of two different heavy quarks. It is also the only meson in which decays of both constituents compete with each other. Numerous predictions for B_c^+ branching fractions have been published (for a review see, e.g., Ref. [2]). To date, no measurements exist which would allow us to test these predictions, even in ratios. Production rates for B_c^+ mesons are about 3 orders of magnitude smaller at high energy colliders than for the other B mesons composed of a b quark and a light quark (B^+ , B^0 , and B_s^0). All experimental knowledge on the B_c^+ meson was obtained from measurements at the Tevatron. It was discovered by the CDF experiment in the semileptonic decay, $B_c^+ \rightarrow J/\psi l^+ \nu_X$ [3]. This decay mode was later used to measure the B_c^+ lifetime [4,5], which is 3 times shorter than that of the other B mesons as both b and c quark may decay. Only one hadronic decay mode of B_c^+ was observed so far, $B_c^+ \rightarrow J/\psi \pi^+$. It was utilized by CDF [6] and DØ [7] to measure the B_c^+ mass [8] to be $6277 \pm 6 \text{ MeV}$ [9].

In this Letter, we present the first observation of the decay mode $B_c^+ \rightarrow J/\psi \pi^+ \pi^- \pi^+$ using a data sample corresponding to an integrated luminosity of 0.8 fb^{-1} collected in 2011 by the LHCb detector [10], in pp collisions at the LHC at $\sqrt{s} = 7 \text{ TeV}$. The branching fraction for this decay is expected to be 1.5–2.3 times higher than that for $B_c^+ \rightarrow J/\psi \pi^+$ [11,12]. However, the larger number of pions in the final state results in a smaller total detection efficiency due to limited detector acceptance. We measure the $B_c^+ \rightarrow J/\psi \pi^+ \pi^- \pi^+$ branching fraction relative to that for the $B_c^+ \rightarrow J/\psi \pi^+$ decay and test the above theoretical predictions.

The LHCb detector [10] is a single-arm forward spectrometer covering the pseudorapidity range $2 < \eta < 5$,

designed for the study of particles containing b or c quarks. The detector includes a high precision tracking system consisting of a silicon-strip vertex detector surrounding the pp interaction region, a large-area silicon-strip detector located upstream of a dipole magnet with a bending power of about 4 Tm, and three stations of silicon-strip detectors and straw drift tubes placed downstream. The combined tracking system has a momentum resolution $\Delta p/p$ that varies from 0.4% at 5 GeV to 0.6% at 100 GeV, and an impact parameter (IP) resolution of $20 \mu\text{m}$ for tracks with high transverse momentum. Charged hadrons are identified using two ring-imaging Cherenkov detectors. Photon, electron, and hadron candidates are identified by a calorimeter system consisting of scintillating-pad and preshower detectors, an electromagnetic calorimeter and a hadronic calorimeter. Muons are identified by a muon system composed of alternating layers of iron and multiwire proportional chambers. The muon system, electromagnetic and hadron calorimeters provide the capability of first-level hardware triggering. The single and dimuon hardware triggers provide good efficiency for $B_c^+ \rightarrow J/\psi \pi^+ [\pi^- \pi^+]$, $J/\psi \rightarrow \mu^+ \mu^-$ events. Here, $\pi^+ [\pi^- \pi^+]$ stands for either π^+ or $\pi^+ \pi^- \pi^+$ depending on the B_c^+ decay mode. Events passing the hardware trigger are read out and sent to an event-filter farm for further processing. Here, a software-based two-stage trigger reduces the rate from 1 MHz to about 3 kHz. The most efficient software triggers [13] for this analysis require a charged track with transverse momentum (p_T) of more than 1.7 GeV ($p_T > 1.0 \text{ GeV}$ if identified as a muon) and with an IP to any primary pp -interaction vertex (PV) larger than $100 \mu\text{m}$. A dimuon trigger requiring $p_T(\mu) > 0.5 \text{ GeV}$, large dimuon mass, $M(\mu^+ \mu^-) > 2.7 \text{ GeV}$, and with no IP requirement complements the single track triggers. At the final stage, we either require a $J/\psi \rightarrow \mu^+ \mu^-$ candidate with $p_T > 2.7 \text{ GeV}$ ($> 1.5 \text{ GeV}$ in the first 42% of data) or a muon-track pair with significant IP.

In the subsequent offline analysis of the data, $J/\psi \rightarrow \mu^+ \mu^-$ candidates are selected with the following criteria: $p_T(\mu) > 0.9 \text{ GeV}$, $p_T(J/\psi) > 3.0 \text{ GeV}$ ($> 1.5 \text{ GeV}$ in the first 42% of data), χ^2 per degree of freedom of the two muons forming a common vertex, $\chi^2_{\text{vtx}}(\mu^+ \mu^-)/\text{ndf} < 9$,

*Full author list given at the end of the article.

and a mass window $3.04 < M(\mu^+ \mu^-) < 3.14$ GeV. We then find $\pi^+ \pi^- \pi^+$ combinations consistent with originating from a common π vertex with $\chi_{\text{vtx}}^2(\pi^+ \pi^- \pi^+)/\text{ndf} < 9$, with each pion separated from all PVs by at least 3 standard deviations ($\chi_{\text{IP}}^2(\pi) > 9$), and having $p_T(\pi) > 0.25$ GeV. A loose kaon veto is applied using the particle identification system. A five-track $J/\psi \pi^+ \pi^- \pi^+$ vertex is formed ($\chi_{\text{vtx}}^2(J/\psi \pi^+ \pi^- \pi^+)/\text{ndf} < 9$). To look for candidates in the normalization mode, $B_c^+ \rightarrow J/\psi \pi^+$, the criteria $p_T(\pi) > 1.5$ GeV and $\chi_{\text{vtx}}^2(J/\psi \pi^+)/\text{ndf} < 16$ are used. All B_c^+ candidates are required to have $p_T > 4.0$ GeV and a decay time of at least 0.25 ps. If more than one PV is reconstructed, the one with the smallest IP significance for the B_c^+ candidate is chosen. The invariant mass of a $\mu^+ \mu^- \pi^+[\pi^- \pi^+]$ combination is evaluated after the muon pair is constrained to the J/ψ mass and all final state particles are constrained to form a common vertex.

Further background suppression is provided by an event selection based on a likelihood ratio. In the case of uncorrelated input variables, this provides the most efficient discrimination between signal and background. The overall likelihood is a product of the probability density functions (PDFs), $\mathcal{P}(x_i)$, for the four sensitive variables (x_i): smallest $\chi_{\text{IP}}^2(\pi)$ among the pion candidates, $\chi_{\text{vtx}}^2(J/\psi \pi^+[\pi^- \pi^+])/\text{ndf}$, B_c^+ candidate IP significance, $\chi_{\text{IP}}^2(B_c)$, and cosine of the largest opening angle between the J/ψ and pion candidates in the plane transverse to the beam. The latter peaks at positive values for the signal as the B_c^+ meson has a high transverse momentum. Background events that combine particles from two different B mesons peak at negative values, while background events that include random combinations of tracks are uniformly distributed. The signal PDFs, $\mathcal{P}_{\text{sig}}(x_i)$, are obtained from a Monte Carlo simulation of $B_c^+ \rightarrow J/\psi \pi^+[\pi^- \pi^+]$ decays. The background PDFs, $\mathcal{P}_{\text{bkg}}(x_i)$, are obtained from the data with a $J/\psi \pi^+[\pi^- \pi^+]$ invariant mass in the range 5.35–5.80 GeV or 6.80–8.50 GeV (far sidebands).

We form the logarithm of the ratio of the signal and background PDFs, $\text{DLL}_{\text{sig/bkg}} = -2 \sum_{i=1}^4 \ln(\mathcal{P}_{\text{sig}}(x_i)/\mathcal{P}_{\text{bkg}}(x_i))$, and require $\text{DLL}_{\text{sig/bkg}} < -5$ for $B_c^+ \rightarrow J/\psi \pi^+ \pi^- \pi^+$ and $\text{DLL}_{\text{sig/bkg}} < -1$ for $B_c^+ \rightarrow J/\psi \pi^+$. These requirements have been chosen to maximize $N_{\text{sig}}/\sqrt{N_{\text{sig}} + N_{\text{bkg}}}$, where N_{sig} is the expected $B_c^+ \rightarrow J/\psi \pi^+[\pi^- \pi^+]$ signal yield and the N_{bkg} is the background yield in the B_c^+ peak region ($\pm 2.5\sigma$). The absolute normalization of N_{sig} and N_{bkg} is obtained from a fit to the $J/\psi \pi^+[\pi^- \pi^+]$ invariant-mass distribution with $\text{DLL}_{\text{sig/bkg}} < 0$, while their dependence on the $\text{DLL}_{\text{sig/bkg}}$ requirement comes from the signal simulation and the far-sidebands, respectively. The $J/\psi \pi^+[\pi^- \pi^+]$ mass distributions after applying all requirements are shown in Fig. 1. To determine the signal yields, a Gaussian signal shape with mass and width as free parameters is fitted to these distributions on top of a background assumed to be an

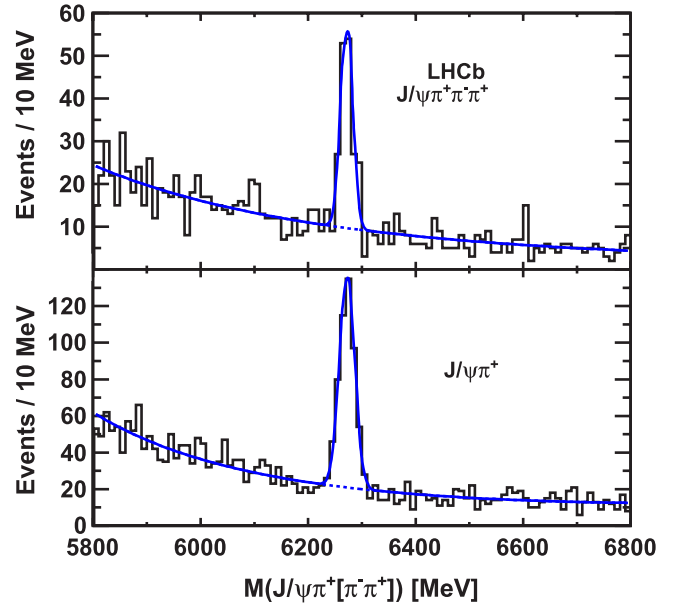


FIG. 1 (color online). Invariant-mass distribution of $B_c^+ \rightarrow J/\psi \pi^+ \pi^- \pi^+$ (top) and $B_c^+ \rightarrow J/\psi \pi^+$ (bottom) candidates. The maximum likelihood fits of B_c^+ signals are superimposed.

exponential function with a second order polynomial as argument. We observe 135 ± 14 $B_c^+ \rightarrow J/\psi \pi^+ \pi^- \pi^+$ and 414 ± 25 $B_c^+ \rightarrow J/\psi \pi^+$ signal events. Using different signal and background parameterizations in the fits, the ratio of the signal yields changes by up to 3%.

The ratio of event yields is converted into a measurement of the branching fraction ratio $\mathcal{B}(B_c^+ \rightarrow J/\psi \pi^+ \pi^- \pi^+)/\mathcal{B}(B_c^+ \rightarrow J/\psi \pi^+)$, where we rely on the simulation for the determination of the ratio of event selection efficiencies. The production of B_c^+ mesons is simulated using the BCVEGPY generator [14,15] which gives a good description of the observed transverse momentum and pseudorapidity (η) distributions in our data. The simulation of the two-body $B_c^+ \rightarrow J/\psi \pi^+$ decay takes into account the spins of the particles and contains no ambiguities. The phenomenological model by Berezhnoy, Likhoded, and Luchinsky [12,16] (BLL) is used to simulate $B_c^+ \rightarrow J/\psi \pi^+ \pi^- \pi^+$ decays. This model, which is based on amplitude factorisation into hadronic and weak currents, implements $B_c^+ \rightarrow J/\psi W^{*+}$ axial-vector form factors and a $W^{*+} \rightarrow \pi^+ \pi^- \pi^+$ decay via the exchange of the virtual $a_1^+(1260)$ decaying via $\rho^0(770)$ and $\rho^0(1450)$ resonances. Since it is not possible to identify which of the same-sign pions originates from the ρ^0 decay, the two ρ^0 paths interfere. To explore the model dependence of the efficiency we also use two phase-space models, implementing $a_1^+(1260) \rightarrow \rho^0(770) \pi^+$ decay with no interference and with either no polarization in the decay (PH) or helicity amplitudes of 0.46, 0.87, and 0.20 for +1, 0 and -1 J/ψ helicities (PHPOL), respectively. For the helicity structure in the PHPOL model, we

use the expectation for the $B^+ \rightarrow D^{*0} a_1^+(1260)$ decay based on Ref. [17]. The background-subtracted distribution [18] of the $M(\pi^+ \pi^- \pi^+)$ mass for the $B_c^+ \rightarrow J/\psi \pi^+ \pi^- \pi^+$ data shown in Fig. 2 exhibits an $a_1^+(1260)$ peak and favors the BLL model. The $\rho^0(770)$ peak in the $M(\pi^+ \pi^-)$ mass distribution shown in Fig. 3 is smaller than that in the two phase-space models, but more pronounced than in the BLL model, with the tail favoring the BLL model. The J/ψ helicity angle distribution shown in Fig. 4 disfavours the model with no polarization. Since the BLL model gives the best overall description of the data, we choose it to evaluate the central value of the ratio of $B_c^+ \rightarrow J/\psi \pi^+ \pi^- \pi^+$ to $B_c^+ \rightarrow J/\psi \pi^+$ efficiencies, 0.135 ± 0.004 , and use the phase-space models to quantify systematic uncertainties. The phase-space models produce relative efficiencies different by -9% (PHPOL) and $+5\%$ (PH). We assign a 9% systematic uncertainty to the model dependence of $B_c^+ \rightarrow J/\psi \pi^+ \pi^- \pi^+$ efficiency.

The distribution of the $M(J/\psi \pi^+ \pi^-)$ mass has an isolated peak of four events at the $\psi(2S)$ mass. From the B_c^+ sidebands we expect 0.50 ± 0.25 background events in this peak. This is consistent with 3.6 ± 0.6 expected $B_c^+ \rightarrow \psi(2S) \pi^+$ events, assuming $\mathcal{B}(B_c^+ \rightarrow \psi(2S) \pi^+) / \mathcal{B}(B_c^+ \rightarrow J/\psi \pi^+)$ equals to $\mathcal{B}(B^+ \rightarrow \psi(2S) \pi^+) / \mathcal{B}(B^+ \rightarrow J/\psi \pi^+) = 0.52 \pm 0.07$ [9] after subtracting 10% to account for the phase-space difference. Since this contribution is only $(2.6 \pm 1.5)\%$ of the $B_c^+ \rightarrow J/\psi \pi^+ \pi^- \pi^+$ signal yield, we do not subtract it and assign a 2% systematic

uncertainty to the ratio of the branching fractions due to the efficiency difference between the $B_c^+ \rightarrow J/\psi a_1(1260)$ and $B_c^+ \rightarrow \psi(2S) \pi^+$, $\psi(2S) \rightarrow J/\psi \pi^+ \pi^-$ decays, as obtained from the simulation.

To test systematic uncertainty in the simulation of $p_T(B_c^+)$, we have calculated weighted averages of efficiency-corrected signal yields in bins of p_T instead of using p_T -integrated yields. The ratio of the branching fractions changes by 2.1% . A similar exercise performed in $\eta(B_c^+)$ bins results in 2.4% change. The result changes by 4% when varying the B_c^+ lifetime assumed in the simulation within its uncertainty [9]. Uncertainty in the simulation of charged tracking efficiency has been studied by comparing the data and simulations in track p_T and η bins on inclusive $J/\psi \rightarrow \mu^+ \mu^-$ signal reconstructed without use of the tracking detectors for one of the muons and then propagated to the final states studied here. Additional uncertainty due to hadronic interactions of charged pions with the detector material has been added. After partial cancellations in the branching fraction ratio, the charged tracking uncertainty is 5% . We have estimated uncertainty due to the trigger simulations to be less than 4% by comparing the data and the simulations on $B^+ \rightarrow J/\psi K^+[\pi^+ \pi^-]$ events triggered independently of the signal particles. The branching fraction ratio changes by $-0.7 \pm 4.8\%$ when the kaon veto is removed, from which we assign 5% systematic uncertainty to it. Summing all

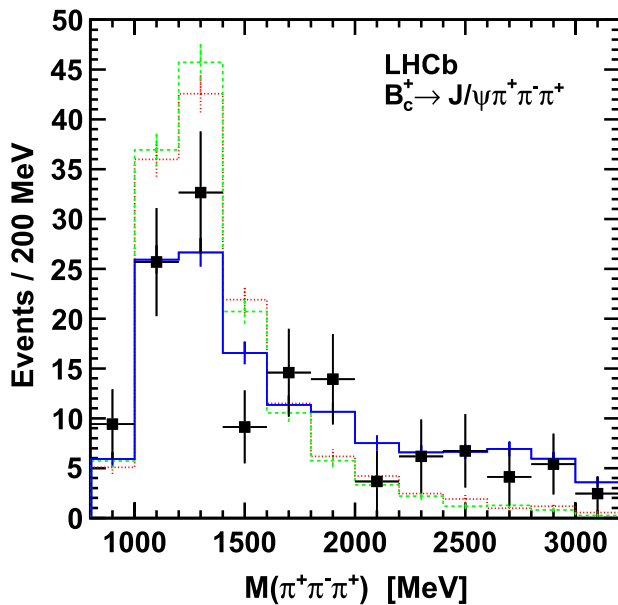


FIG. 2 (color online). Invariant-mass distribution of the $\pi^+ \pi^- \pi^+$ combinations for the sideband-subtracted $B_c^+ \rightarrow J/\psi \pi^+ \pi^- \pi^+$ data (points) and signal simulation (lines). The solid blue line corresponds to the BLL simulations, the PH model is shown as a green dashed line and the PHPOL model is shown as a red dotted line. All error bars are statistical.

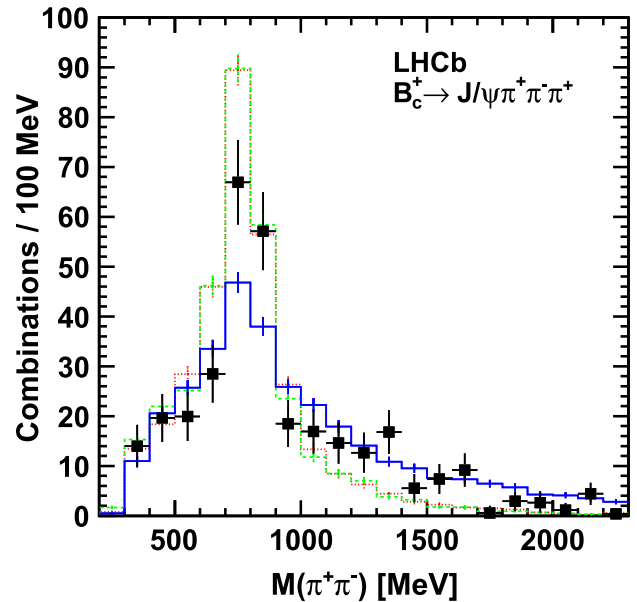


FIG. 3 (color online). Invariant-mass distribution of the $\pi^+ \pi^-$ combinations (two entries per B_c^+ candidate) for the sideband-subtracted $B_c^+ \rightarrow J/\psi \pi^+ \pi^- \pi^+$ data (points) and signal simulation (lines). The solid blue line corresponds to the BLL simulations, the PH model is shown as a green dashed line and the PHPOL model is shown as a red dotted line. All error bars are statistical.

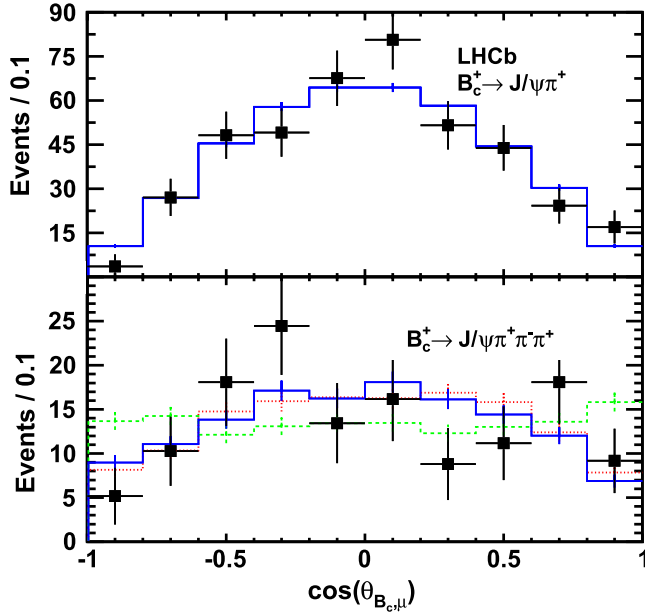


FIG. 4 (color online). Distributions of the cosine of the angle between the μ^+ and B_c^+ boosted to the rest frame of the J/ψ meson for the sideband-subtracted $B_c^+ \rightarrow J/\psi \pi^+$ (top) and $B_c^+ \rightarrow J/\psi \pi^+ \pi^- \pi^+$ (bottom) data (points) and signal simulation (lines). In the bottom plot, the solid blue line corresponds to the BLL simulations, the PH model is shown as a green dashed line and the PHPOL model is shown as a red dotted line. All error bars are statistical.

contributions in quadrature, the total systematic error on the branching fraction ratio amounts to 14%. As a result, we measure the branching fraction ratio

$$\frac{\mathcal{B}(B_c^+ \rightarrow J/\psi \pi^+ \pi^- \pi^+)}{\mathcal{B}(B_c^+ \rightarrow J/\psi \pi^+)} = 2.41 \pm 0.30 \pm 0.33,$$

where the first uncertainty is statistical and the second systematic.

The obtained result can be compared to theoretical predictions; these assume factorisation into $B_c^+ \rightarrow J/\psi W^{+*}$ and $W^{+*} \rightarrow \pi^+[\pi^- \pi^+]$. The contributions of strong interactions to $B_c^+ \rightarrow J/\psi W^{+*}$ are included in form-factors which can be calculated in various approaches such as a nonrelativistic quark model or sum rules. The coupling of a single pion to a W^{+*} is described by the pion decay constant. The coupling of three pions to a W^{+*} is measured in $\tau^- \rightarrow \nu_\tau \pi^- \pi^+ \pi^-$ decays, which are dominated by the $a_1(1260)$ resonance. The prediction by Rakitin and Koshkarev, using the no-recoil approximation in $B_c^+ \rightarrow J/\psi W^{+*}$, is $\mathcal{B}(B_c^+ \rightarrow J/\psi \pi^+ \pi^- \pi^+)/\mathcal{B}(B_c^+ \rightarrow J/\psi \pi^+) = 1.5$ [11]. Likhoded and Luchinsky used three different approaches to predict the form factors and obtained $\mathcal{B}(B_c^+ \rightarrow J/\psi \pi^+ \pi^- \pi^+)/\mathcal{B}(B_c^+ \rightarrow J/\psi \pi^+) = 1.9, 2.0,$ and $2.3,$ respectively [12]. Our result prefers the latter predictions. It is also consistent with

$\mathcal{B}(B^+ \rightarrow \bar{D}^{*0} \pi^+ \pi^- \pi^+)/\mathcal{B}(B^+ \rightarrow \bar{D}^{*0} \pi^+) = 2.0 \pm 0.3$ [9], which is mediated by similar decay mechanisms, and with a similar ratio of phase-space factors. Our result constitutes the first test of theoretical predictions for branching fractions of B_c^+ decays.

We express our gratitude to our colleagues in the CERN accelerator departments for the excellent performance of the LHC. We thank the technical and administrative staff at CERN and at the LHCb institutes, and acknowledge support from the National Agencies: CAPES, CNPq, FAPERJ and FINEP (Brazil); CERN; NSFC (China); CNRS/IN2P3 (France); BMBF, DFG, HGF and MPG (Germany); SFI (Ireland); INFN (Italy); FOM and NWO (The Netherlands); SCSR (Poland); ANCS (Romania); MinES of Russia and Rosatom (Russia); MICINN, XuntaGal and GENCAT (Spain); SNSF and SER (Switzerland); NAS Ukraine (Ukraine); STFC (United Kingdom); NSF (USA). We also acknowledge the support received from the ERC under FP7 and the Region Auvergne.

- [1] Charge-conjugate states are implied in this Letter.
- [2] N. Brambilla *et al.* (Quarkonium Working Group) CERN Yellow Report, Report No. CERN-2005-005.
- [3] F. Abe *et al.* (CDF Collaboration), *Phys. Rev. Lett.* **81**, 2432 (1998).
- [4] A. Abulencia *et al.* (CDF Collaboration), *Phys. Rev. Lett.* **97**, 012002 (2006).
- [5] V. M. Abazov *et al.* (DØ Collaboration), *Phys. Rev. Lett.* **102**, 092001 (2009).
- [6] T. Aaltonen *et al.* (CDF Collaboration), *Phys. Rev. Lett.* **100**, 182002 (2008).
- [7] V. M. Abazov *et al.* (DØ Collaboration), *Phys. Rev. Lett.* **101**, 012001 (2008).
- [8] We use mass and momentum units in which $c = 1$.
- [9] K. Nakamura *et al.* (Particle Data Group), *J. Phys. G* **37**, 075021 (2010).
- [10] A. A. Alves, Jr. *et al.* (LHCb Collaboration) *JINST* **3**, S08005 (2008).
- [11] A. Rakitin and S. Koshkarev, *Phys. Rev. D* **81**, 014005 (2010).
- [12] A. K. Likhoded and A. V. Luchinsky, *Phys. Rev. D* **81**, 014015 (2010).
- [13] V. Gligorov, C. Thomas, and M. Williams, CERN Report No. LHCb-PUB-2011-016.
- [14] C.-H. Chang, C. Driouichi, P. Eerola, and X.G. Wu, *Comput. Phys. Commun.* **159**, 192 (2004).
- [15] C.-H. Chang, J.-X. Wang, and X.-G. Wu, *Comput. Phys. Commun.* **175**, 624 (2006).
- [16] A. Berezhnoy, A. Likhoded, and A. Luchinsky, [arXiv:1104.0808](https://arxiv.org/abs/1104.0808).
- [17] J. L. Rosner, *Phys. Rev. D* **42**, 3732 (1990).
- [18] For comparisons between the data and simulation we use the data within $\pm 2.5\sigma$ of the observed peak position in the B_c^+ mass (signal region). We subtract the background distributions as estimated from the $\pm(5 - 30)\sigma$ near sidebands.

R. Aaij,³⁸ C. Abellan Beteta,^{33,n} B. Adeva,³⁴ M. Adinolfi,⁴³ C. Adrover,⁶ A. Affolder,⁴⁹ Z. Ajaltouni,⁵ J. Albrecht,³⁵ F. Alessio,³⁵ M. Alexander,⁴⁸ S. Ali,³⁸ G. Alkhazov,²⁷ P. Alvarez Cartelle,³⁴ A. A. Alves, Jr.,²² S. Amato,² Y. Amhis,³⁶ J. Anderson,³⁷ R. B. Appleby,⁵¹ O. Aquines Gutierrez,¹⁰ F. Archilli,^{18,35} A. Artamonov,³² M. Artuso,^{53,35} E. Aslanides,⁶ G. Auriemma,^{22,m} S. Bachmann,¹¹ J. J. Back,⁴⁵ V. Balagura,^{28,35} W. Baldini,¹⁶ R. J. Barlow,⁵¹ C. Barschel,³⁵ S. Barsuk,⁷ W. Barter,⁴⁴ A. Bates,⁴⁸ C. Bauer,¹⁰ Th. Bauer,³⁸ A. Bay,³⁶ I. Bediaga,¹ S. Belogurov,²⁸ K. Belous,³² I. Belyaev,²⁸ E. Ben-Haim,⁸ M. Benayoun,⁸ G. Bencivenni,¹⁸ S. Benson,⁴⁷ J. Benton,⁴³ R. Bernet,³⁷ M.-O. Bettler,¹⁷ M. van Beuzekom,³⁸ A. Bien,¹¹ S. Bifani,¹² T. Bird,⁵¹ A. Bizzeti,^{17,h} P. M. Bjørnstad,⁵¹ T. Blake,³⁵ F. Blanc,³⁶ C. Blanks,⁵⁰ J. Blouw,¹¹ S. Blusk,⁵³ A. Bobrov,³¹ V. Bocci,²² A. Bondar,³¹ N. Bondar,²⁷ W. Bonivento,¹⁵ S. Borghi,^{48,51} A. Borgia,⁵³ T. J. V. Bowcock,⁴⁹ C. Bozzi,¹⁶ T. Brambach,⁹ J. van den Brand,³⁹ J. Bressieux,³⁶ D. Brett,⁵¹ M. Britsch,¹⁰ T. Britton,⁵³ N. H. Brook,⁴³ H. Brown,⁴⁹ A. Büchler-Germann,³⁷ I. Burducea,²⁶ A. Bursche,³⁷ J. Buytaert,³⁵ S. Cadetdu,¹⁵ O. Callot,⁷ M. Calvi,^{20,j} M. Calvo Gomez,^{33,n} A. Camboni,³³ P. Campana,^{18,35} A. Carbone,¹⁴ G. Carboni,^{21,k} R. Cardinale,^{19,35,i} A. Cardini,¹⁵ L. Carson,⁵⁰ K. Carvalho Akiba,² G. Casse,⁴⁹ M. Cattaneo,³⁵ Ch. Cauet,⁹ M. Charles,⁵² Ph. Charpentier,³⁵ N. Chiapolini,³⁷ K. Ciba,³⁵ X. Cid Vidal,³⁴ G. Ciezarek,⁵⁰ P. E. L. Clarke,⁴⁷ M. Clemencic,³⁵ H. V. Cliff,⁴⁴ J. Closier,³⁵ C. Coca,²⁶ V. Coco,³⁸ J. Cogan,⁶ P. Collins,³⁵ A. Comerma-Montells,³³ A. Contu,⁵² A. Cook,⁴³ M. Coombes,⁴³ G. Corti,³⁵ B. Couturier,³⁵ G. A. Cowan,³⁶ R. Currie,⁴⁷ C. D'Ambrosio,³⁵ P. David,⁸ P. N. Y. David,³⁸ I. De Bonis,⁴ K. De Bruyn,³⁸ S. De Capua,^{21,k} M. De Cian,³⁷ J. M. De Miranda,¹ L. De Paula,² P. De Simone,¹⁸ D. Decamp,⁴ M. Deckenhoff,⁹ H. Degaudenzi,^{36,35} L. Del Buono,⁸ C. Deplano,¹⁵ D. Derkach,^{14,35} O. Deschamps,⁵ F. Dettori,³⁹ J. Dickens,⁴⁴ H. Dijkstra,³⁵ P. Diniz Batista,¹ F. Domingo Bonal,^{33,n} S. Donleavy,⁴⁹ F. Dordei,¹¹ A. Dosi Suárez,³⁴ D. Dossett,⁴⁵ A. Dovbnya,⁴⁰ F. Dupertuis,³⁶ R. Dzhelyadin,³² A. Dziurda,²³ S. Easo,⁴⁶ U. Egede,⁵⁰ V. Egorychev,²⁸ S. Eidelman,³¹ D. van Eijk,³⁸ F. Eisele,¹¹ S. Eisenhardt,⁴⁷ R. Ekelhof,⁹ L. Eklund,⁴⁸ Ch. Elsasser,³⁷ D. Elsby,⁴² D. Esperante Pereira,³⁴ A. Falabella,^{16,14,d} C. Färber,¹¹ G. Fardell,⁴⁷ C. Farinelli,³⁸ S. Farry,¹² V. Fave,³⁶ V. Fernandez Albor,³⁴ M. Ferro-Luzzi,³⁵ S. Filippov,³⁰ C. Fitzpatrick,⁴⁷ M. Fontana,¹⁰ F. Fontanelli,^{19,i} R. Forty,³⁵ O. Francisco,² M. Frank,³⁵ C. Frei,³⁵ M. Frosini,^{17,f} S. Furcas,²⁰ A. Gallas Torreira,³⁴ D. Galli,^{14,c} M. Gandelman,² P. Gandini,⁵² Y. Gao,³ J.-C. Garnier,³⁵ J. Garofoli,⁵³ J. Garra Tico,⁴⁴ L. Garrido,³³ D. Gascon,³³ C. Gaspar,³⁵ R. Gauld,⁵² N. Gauvin,³⁶ M. Gersabeck,³⁵ T. Gershon,^{45,35} Ph. Ghez,⁴ V. Gibson,⁴⁴ V. V. Gligorov,³⁵ C. Göbel,⁵⁴ D. Golubkov,²⁸ A. Golutvin,^{50,28,35} A. Gomes,² H. Gordon,⁵² M. Grabalosa Gándara,³³ R. Graciani Diaz,³³ L. A. Granado Cardoso,³⁵ E. Graugés,³³ G. Graziani,¹⁷ A. Grecu,²⁶ E. Greening,⁵² S. Gregson,⁴⁴ B. Gui,⁵³ E. Gushchin,³⁰ Yu. Guz,³² T. Gys,³⁵ C. Hadjivasiliou,⁵³ G. Haefeli,³⁶ C. Haen,³⁵ S. C. Haines,⁴⁴ T. Hampson,⁴³ S. Hansmann-Menzemer,¹¹ R. Harji,⁵⁰ N. Harnew,⁵² J. Harrison,⁵¹ P. F. Harrison,⁴⁵ T. Hartmann,⁵⁵ J. He,⁷ V. Heijne,³⁸ K. Hennessy,⁴⁹ P. Henrard,⁵ J. A. Hernandez Morata,³⁴ E. van Herwijnen,³⁵ E. Hicks,⁴⁹ K. Holubyev,¹¹ P. Hopchev,⁴ W. Hulsbergen,³⁸ P. Hunt,⁵² T. Huse,⁴⁹ R. S. Huston,¹² D. Hutchcroft,⁴⁹ D. Hynds,⁴⁸ V. Iakovenko,⁴¹ P. Ilten,¹² J. Imong,⁴³ R. Jacobsson,³⁵ A. Jaeger,¹¹ M. Jahjah Hussein,⁵ E. Jans,³⁸ F. Jansen,³⁸ P. Jaton,³⁶ B. Jean-Marie,⁷ F. Jing,³ M. John,⁵² D. Johnson,⁵² C. R. Jones,⁴⁴ B. Jost,³⁵ M. Kabbalo,⁹ S. Kandybei,⁴⁰ M. Karacson,³⁵ T. M. Karbach,⁹ J. Keaveney,¹² I. R. Kenyon,⁴² U. Kerzel,³⁵ T. Ketel,³⁹ A. Keune,³⁶ B. Khanji,⁶ Y. M. Kim,⁴⁷ M. Knecht,³⁶ R. F. Koopman,³⁹ P. Koppenburg,³⁸ M. Korolev,²⁹ A. Kozlinskiy,³⁸ L. Kravchuk,³⁰ K. Kreplin,¹¹ M. Kreps,⁴⁵ G. Krocker,¹¹ P. Krokovny,³¹ F. Kruse,⁹ K. Kruzelecki,³⁵ M. Kucharczyk,^{20,23,35,j} V. Kudryavtsev,³¹ T. Kvaratskheliya,^{28,35} V. N. La Thi,³⁶ D. Lacarrere,³⁵ G. Lafferty,⁵¹ A. Lai,¹⁵ D. Lambert,⁴⁷ R. W. Lambert,³⁹ E. Lanciotti,³⁵ G. Lanfranchi,¹⁸ C. Langenbruch,³⁵ T. Latham,⁴⁵ C. Lazzeroni,⁴² R. Le Gac,⁶ J. van Leerdam,³⁸ J.-P. Lees,⁴ R. Lefèvre,⁵ A. Leflat,^{29,35} J. Lefrançois,⁷ O. Leroy,⁶ T. Lesiak,²³ L. Li,³ L. Li Gioi,⁵ M. Lieng,⁹ M. Liles,⁴⁹ R. Lindner,³⁵ C. Linn,¹¹ B. Liu,³ G. Liu,³⁵ J. von Loeben,²⁰ J. H. Lopes,² E. Lopez Asamar,³³ N. Lopez-March,³⁶ H. Lu,³ J. Luisier,³⁶ A. Mac Raighne,⁴⁸ F. Machefert,⁷ I. V. Machikhiliyan,^{4,28} F. Maciuc,¹⁰ O. Maev,^{27,35} J. Magnin,¹ S. Malde,⁵² R. M. D. Mamunur,³⁵ G. Manca,^{15,d} G. Mancinelli,⁶ N. Mangiafave,⁴⁴ U. Marconi,¹⁴ R. Märki,³⁶ J. Marks,¹¹ G. Martellotti,²² A. Martens,⁸ L. Martin,⁵² A. Martín Sánchez,⁷ M. Martinelli,³⁸ D. Martinez Santos,³⁵ A. Massafferri,¹ Z. Mathe,¹² C. Matteuzzi,²⁰ M. Matveev,²⁷ E. Maurice,⁶ B. Maynard,⁵³ A. Mazurov,^{16,30,35} G. McGregor,⁵¹ R. McNulty,¹² M. Meissner,¹¹ M. Merk,³⁸ J. Merkel,⁹ S. Miglioranza,³⁵ D. A. Milanes,¹³ M.-N. Minard,⁴ J. Molina Rodriguez,⁵⁴ S. Monteil,⁵ D. Moran,¹² P. Morawski,²³ R. Mountain,⁵³ I. Mous,³⁸ F. Muheim,⁴⁷ K. Müller,³⁷ R. Muresan,²⁶ B. Muryn,²⁴ B. Muster,³⁶ J. Mylroie-Smith,⁴⁹ P. Naik,⁴³ T. Nakada,³⁶ R. Nandakumar,⁴⁶ I. Nasteva,¹ M. Needham,⁴⁷ N. Neufeld,³⁵ A. D. Nguyen,³⁶

C. Nguyen-Mau,^{36,o} M. Nicol,⁷ V. Niess,⁵ N. Nikitin,²⁹ T. Nikodem,¹¹ A. Nomerotski,^{52,35} A. Novoselov,³² A. Oblakowska-Mucha,²⁴ V. Obraztsov,³² S. Oggero,³⁸ S. Ogilvy,⁴⁸ O. Okhrimenko,⁴¹ R. Oldeman,^{15,35,d} M. Orlandea,²⁶ J. M. Otalora Goicochea,² P. Owen,⁵⁰ B. K. Pal,⁵³ J. Palacios,³⁷ A. Palano,^{13,b} M. Palutan,¹⁸ J. Panman,³⁵ A. Papanestis,⁴⁶ M. Pappagallo,⁴⁸ C. Parkes,⁵¹ C. J. Parkinson,⁵⁰ G. Passaleva,¹⁷ G. D. Patel,⁴⁹ M. Patel,⁵⁰ S. K. Paterson,⁵⁰ G. N. Patrick,⁴⁶ C. Patrignani,^{19,i} C. Pavel-Nicorescu,²⁶ A. Pazos Alvarez,³⁴ A. Pellegrino,³⁸ G. Penso,^{22,l} M. Pepe Altarelli,³⁵ S. Perazzini,^{14,c} D. L. Perego,^{20,j} E. Perez Trigo,³⁴ A. Pérez-Calero Yzquierdo,³³ P. Perret,⁵ M. Perrin-Terrin,⁶ G. Pessina,²⁰ A. Petrolini,^{19,i} A. Phan,⁵³ E. Picatoste Olloqui,³³ B. Pie Valls,³³ B. Pietrzyk,⁴ T. Pilař,⁴⁵ D. Pinci,²² R. Plackett,⁴⁸ S. Playfer,⁴⁷ M. Plo Casasus,³⁴ G. Polok,²³ A. Poluektov,^{45,31} E. Polcarpo,² D. Popov,¹⁰ B. Popovici,²⁶ C. Potterat,³³ A. Powell,⁵² J. Prisciandaro,³⁶ V. Pugatch,⁴¹ A. Puig Navarro,³³ W. Qian,⁵³ J. H. Rademacker,⁴³ B. Rakotomiaramanana,³⁶ M. S. Rangel,² I. Raniuk,⁴⁰ G. Raven,³⁹ S. Redford,⁵² M. M. Reid,⁴⁵ A. C. dos Reis,¹ S. Ricciardi,⁴⁶ A. Richards,⁵⁰ K. Rinnert,⁴⁹ D. A. Roa Romero,⁵ P. Robbe,⁷ E. Rodrigues,^{48,51} F. Rodrigues,² P. Rodriguez Perez,³⁴ G. J. Rogers,⁴⁴ S. Roiser,³⁵ V. Romanovsky,³² M. Rosello,^{33,n} J. Rouvinet,³⁶ T. Ruf,³⁵ H. Ruiz,³³ G. Sabatino,^{21,k} J. J. Saborido Silva,³⁴ N. Sagidova,²⁷ P. Sail,⁴⁸ B. Saitta,^{15,d} C. Salzmann,³⁷ M. Sannino,^{19,i} R. Santacesaria,²² C. Santamarina Rios,³⁴ R. Santinelli,³⁵ E. Santovetti,^{21,k} M. Sapunov,⁶ A. Sarti,^{18,l} C. Satriano,^{22,m} A. Satta,²¹ M. Savrie,^{16,e} D. Savrina,²⁸ P. Schaack,⁵⁰ M. Schiller,³⁹ H. Schindler,³⁵ S. Schleich,⁹ M. Schlupp,⁹ M. Schmelling,¹⁰ B. Schmidt,³⁵ O. Schneider,³⁶ A. Schopper,³⁵ M.-H. Schune,⁷ R. Schwemmer,³⁵ B. Sciascia,¹⁸ A. Sciubba,^{18,l} M. Seco,³⁴ A. Semennikov,²⁸ K. Senderowska,²⁴ I. Sepp,⁵⁰ N. Serra,³⁷ J. Serrano,⁶ P. Seyfert,¹¹ M. Shapkin,³² I. Shapoval,^{40,35} P. Shatalov,²⁸ Y. Shcheglov,²⁷ T. Shears,⁴⁹ L. Shekhtman,³¹ O. Shevchenko,⁴⁰ V. Shevchenko,²⁸ A. Shires,⁵⁰ R. Silva Coutinho,⁴⁵ T. Skwarnicki,⁵³ N. A. Smith,⁴⁹ E. Smith,^{52,46} K. Sobczak,⁵ F. J. P. Soler,⁴⁸ A. Solomin,⁴³ F. Soomro,^{18,35} B. Souza De Paula,² B. Spaan,⁹ A. Sparkes,⁴⁷ P. Spradlin,⁴⁸ F. Stagni,³⁵ S. Stahl,¹¹ O. Steinkamp,³⁷ S. Stoica,²⁶ S. Stone,^{53,35} B. Storaci,³⁸ M. Straticiu,²⁶ U. Straumann,³⁷ V. K. Subbiah,³⁵ S. Swientek,⁹ M. Szczekowski,²⁵ P. Szczypka,³⁶ T. Szumlak,²⁴ S. T'Jampens,⁴ E. Teodorescu,²⁶ F. Teubert,³⁵ C. Thomas,⁵² E. Thomas,³⁵ J. van Tilburg,¹¹ V. Tisserand,⁴ M. Tobin,³⁷ S. Tolk,³⁹ S. Topp-Joergensen,⁵² N. Torr,⁵² E. Tournefier,^{4,50} S. Tourneur,³⁶ M. T. Tran,³⁶ A. Tsaregorodtsev,⁶ N. Tuning,³⁸ M. Ubeda Garcia,³⁵ A. Ukleja,²⁵ U. Uwer,¹¹ V. Vagnoni,¹⁴ G. Valenti,¹⁴ R. Vazquez Gomez,³³ P. Vazquez Regueiro,³⁴ S. Vecchi,¹⁶ J. J. Velthuis,⁴³ M. Veltri,^{17,g} B. Viaud,⁷ I. Videau,⁷ D. Vieira,² X. Vilasis-Cardona,^{33,n} J. Visniakov,³⁴ A. Vollhardt,³⁷ D. Volyansky,¹⁰ D. Voong,⁴³ A. Vorobyev,²⁷ V. Vorobyev,³¹ H. Voss,¹⁰ R. Waldi,⁵⁵ S. Wandernoth,¹¹ J. Wang,⁵³ D. R. Ward,⁴⁴ N. K. Watson,⁴² A. D. Webber,⁵¹ D. Websdale,⁵⁰ M. Whitehead,⁴⁵ D. Wiedner,¹¹ L. Wiggers,³⁸ G. Wilkinson,⁵² M. P. Williams,^{45,46} M. Williams,⁵⁰ F. F. Wilson,⁴⁶ J. Wishahi,⁹ M. Witek,²³ W. Witzeling,³⁵ S. A. Wotton,⁴⁴ K. Wyllie,³⁵ Y. Xie,⁴⁷ F. Xing,⁵² Z. Xing,⁵³ Z. Yang,³ R. Young,⁴⁷ O. Yushchenko,³² M. Zangoli,¹⁴ M. Zavertyaev,^{10,a} F. Zhang,³ L. Zhang,⁵³ W. C. Zhang,¹² Y. Zhang,³ A. Zhelezov,¹¹ L. Zhong,³ and A. Zvyagin³⁵

(LHCb Collaboration)

¹Centro Brasileiro de Pesquisas Físicas (CBPF), Rio de Janeiro, Brazil²Universidade Federal do Rio de Janeiro (UFRJ), Rio de Janeiro, Brazil³Center for High Energy Physics, Tsinghua University, Beijing, China⁴LAPP, Université de Savoie, CNRS/IN2P3, Annecy-Le-Vieux, France⁵Clermont Université, Université Blaise Pascal, CNRS/IN2P3, LPC, Clermont-Ferrand, France⁶CPPM, Aix-Marseille Université, CNRS/IN2P3, Marseille, France⁷LAL, Université Paris-Sud, CNRS/IN2P3, Orsay, France⁸LPNHE, Université Pierre et Marie Curie, Université Paris Diderot, CNRS/IN2P3, Paris, France⁹Fakultät Physik, Technische Universität Dortmund, Dortmund, Germany¹⁰Max-Planck-Institut für Kernphysik (MPIK), Heidelberg, Germany¹¹Physikalisches Institut, Ruprecht-Karls-Universität Heidelberg, Heidelberg, Germany¹²School of Physics, University College Dublin, Dublin, Ireland¹³Sezione INFN di Bari, Bari, Italy¹⁴Sezione INFN di Bologna, Bologna, Italy¹⁵Sezione INFN di Cagliari, Cagliari, Italy¹⁶Sezione INFN di Ferrara, Ferrara, Italy¹⁷Sezione INFN di Firenze, Firenze, Italy¹⁸Laboratori Nazionali dell'INFN di Frascati, Frascati, Italy¹⁹Sezione INFN di Genova, Genova, Italy

- ²⁰*Sezione INFN di Milano Bicocca, Milano, Italy*
²¹*Sezione INFN di Roma Tor Vergata, Roma, Italy*
²²*Sezione INFN di Roma La Sapienza, Roma, Italy*
²³*Henryk Niewodniczanski Institute of Nuclear Physics Polish Academy of Sciences, Kraków, Poland*
²⁴*AGH University of Science and Technology, Kraków, Poland*
²⁵*Soltan Institute for Nuclear Studies, Warsaw, Poland*
²⁶*Horia Hulubei National Institute of Physics and Nuclear Engineering, Bucharest-Magurele, Romania*
²⁷*Petersburg Nuclear Physics Institute (PNPI), Gatchina, Russia*
²⁸*Institute of Theoretical and Experimental Physics (ITEP), Moscow, Russia*
²⁹*Institute of Nuclear Physics, Moscow State University (SINP MSU), Moscow, Russia*
³⁰*Institute for Nuclear Research of the Russian Academy of Sciences (INR RAN), Moscow, Russia*
³¹*Budker Institute of Nuclear Physics (SB RAS) and Novosibirsk State University, Novosibirsk, Russia*
³²*Institute for High Energy Physics (IHEP), Protvino, Russia*
³³*Universitat de Barcelona, Barcelona, Spain*
³⁴*Universidad de Santiago de Compostela, Santiago de Compostela, Spain*
³⁵*European Organization for Nuclear Research (CERN), Geneva, Switzerland*
³⁶*Ecole Polytechnique Fédérale de Lausanne (EPFL), Lausanne, Switzerland*
³⁷*Physik-Institut, Universität Zürich, Zürich, Switzerland*
³⁸*Nikhef National Institute for Subatomic Physics, Amsterdam, The Netherlands*
³⁹*Nikhef National Institute for Subatomic Physics and VU University Amsterdam, Amsterdam, The Netherlands*
⁴⁰*NSC Kharkiv Institute of Physics and Technology (NSC KIPT), Kharkiv, Ukraine*
⁴¹*Institute for Nuclear Research of the National Academy of Sciences (KINR), Kyiv, Ukraine*
⁴²*University of Birmingham, Birmingham, United Kingdom*
⁴³*H.H. Wills Physics Laboratory, University of Bristol, Bristol, United Kingdom*
⁴⁴*Cavendish Laboratory, University of Cambridge, Cambridge, United Kingdom*
⁴⁵*Department of Physics, University of Warwick, Coventry, United Kingdom*
⁴⁶*STFC Rutherford Appleton Laboratory, Didcot, United Kingdom*
⁴⁷*School of Physics and Astronomy, University of Edinburgh, Edinburgh, United Kingdom*
⁴⁸*School of Physics and Astronomy, University of Glasgow, Glasgow, United Kingdom*
⁴⁹*Oliver Lodge Laboratory, University of Liverpool, Liverpool, United Kingdom*
⁵⁰*Imperial College London, London, United Kingdom*
⁵¹*School of Physics and Astronomy, University of Manchester, Manchester, United Kingdom*
⁵²*Department of Physics, University of Oxford, Oxford, United Kingdom*
⁵³*Syracuse University, Syracuse, New York, USA*
⁵⁴*Pontifícia Universidade Católica do Rio de Janeiro (PUC-Rio), Rio de Janeiro, Brazil (associated to Universidade Federal do Rio de Janeiro (UFRJ), Rio de Janeiro, Brazil)*
⁵⁵*Institut für Physik, Universität Rostock, Rostock, Germany (associated to Physikalisches Institut, Ruprecht-Karls-Universität Heidelberg, Heidelberg, Germany)*

^aAlso at P.N. Lebedev Physical Institute, Russian Academy of Science (LPI RAS), Moscow, Russia.

^bAlso at Università di Bari, Bari, Italy.

^cAlso at Università di Bologna, Bologna, Italy.

^dAlso at Università di Cagliari, Cagliari, Italy.

^eAlso at Università di Ferrara, Ferrara, Italy.

^fAlso at Università di Firenze, Firenze, Italy.

^gAlso at Università di Urbino, Urbino, Italy.

^hAlso at Università Modena e Reggio Emilia, Modena, Italy.

ⁱAlso at Università di Genova, Genova, Italy.

^jAlso at Università di Milano Bicocca, Milano, Italy.

^kAlso at Università di Roma Tor Vergata, Roma, Italy.

^lAlso at Università di Roma La Sapienza, Roma, Italy.

^mAlso at Università della Basilicata, Potenza, Italy.

ⁿAlso at LIFAELS, La Salle, Universitat Ramon Llull, Barcelona, Spain.

^oAlso at Hanoi University of Science, Hanoi, Viet Nam.